cmgh
CELLULAR AND MOLECULAR GASTROENTEROLOGY AND HEPATOLOGY

ORIGINAL RESEARCH

Inhibition of BMP2 and BMP4 Represses Barrett's Esophagus While Enhancing the Regeneration of Squamous Epithelium in Preclinical Models

Ana C. P. Correia,[1,2,*] Danielle Straub,[1,2,*] Matthew Read,[3,4] Sanne J. M. Hoefnagel,[1,2] Salvador Romero-Pinedo,[5,6] Ana C. Abadía-Molina,[5,6] Nicholas J. Clemons,[7,8] Kenneth Wang,[9] Silvia Calpe,[1,2] Wayne Phillips,[7,10] and Kausilia K. Krishnadath[11,12]

[1]Center of Experimental and Molecular Medicine, Amsterdam UMC, University of Amsterdam, Amsterdam, Netherlands; [2]Department of Gastroenterology and Hepatology, Amsterdam UMC, University of Amsterdam, Cancer Center Amsterdam, Amsterdam, the Netherlands; [3]Department of Surgery, St Vincent's Hospital, Melbourne, Victoria, Australia; [4]Department of Surgery, The University of Melbourne, St Vincent's Hospital, Melbourne, Victoria, Australia; [5]Biomedical Research Centre, CIBM, Institute of Biomedicine and Regenerative Investigation, IBIMER, University of Granada, Granada, Spain; [6]Department of Biochemistry and Molecular Biology III and Immunology, University of Granada, Granada, Spain; [7]Sir Peter MacCallum Department of Oncology, The University of Melbourne, Melbourne, Victoria, Australia; [8]Division of Cancer Research, Peter MacCallum Cancer Centre, Melbourne, Australia; [9]Division of Gastroenterology and Hepatology, Mayo Clinic, Rochester, Minnesota; [10]Cancer Biology and Surgical Oncology Research Laboratory, Peter MacCallum Cancer Centre, Melbourne, Victoria, Australia; [11]Department of Gastroenterology and Hepatology, Antwerp University Hospital, Antwerp, Belgium; and [12]Laboratory of Experimental Medicine and Pediatrics, University of Antwerp, Antwerp, Belgium

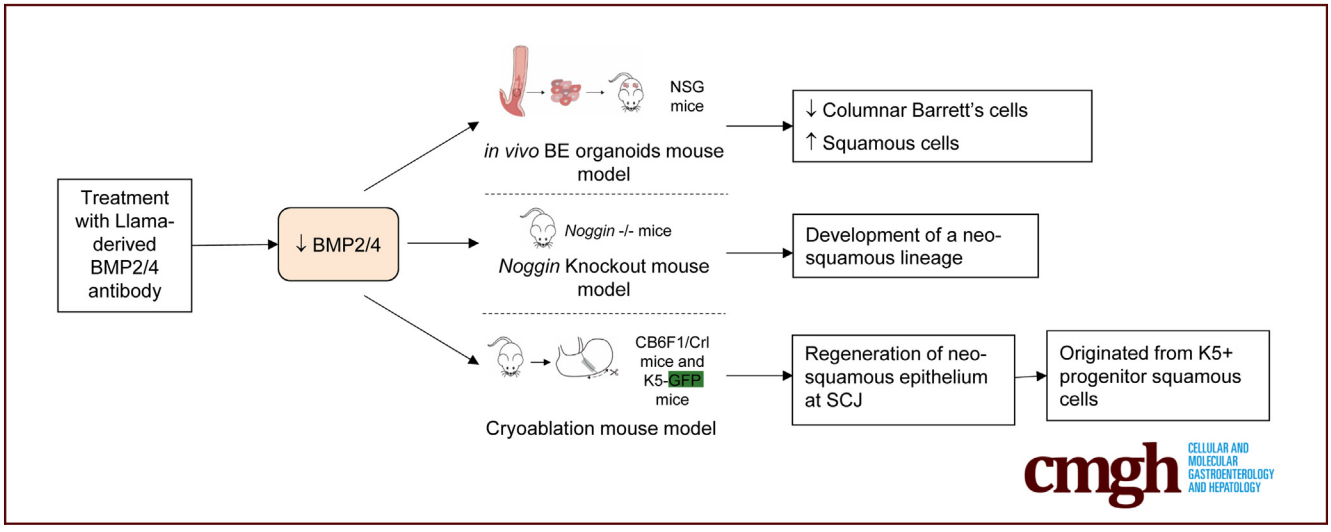

SUMMARY

Targeting the BMP-pSMAD pathway with anti-BMP2/4 inhibitors effectively suppresses Barrett's epithelium and promotes re-epithelialization by squamous cells in different preclinical mouse models of disease. In this study different mouse models were developed to study the efficacy of llama-derived anti-BMP2/4 antibodies. Anti-BMP2/4 antibodies were shown to be an attractive molecular therapeutic option in the treatment of Barrett's esophagus.

BACKGROUND & AIMS: Barrett's esophagus is considered to be a metaplastic lesion that predisposes for esophageal adenocarcinoma. Development of Barrett's esophagus is considered to be driven by sonic hedgehog mediated bone morphogenetic protein (BMP) signaling. We aimed to investigate in preclinical in vivo models whether targeting canonical BMP signaling could be an effective treatment for Barrett's esophagus.

METHODS AND RESULTS: Selective inhibition of BMP2 and BMP4 within an in vivo organoid model of Barrett's esophagus inhibited development of columnar Barrett's cells, while favoring expansion of squamous cells. Silencing of noggin, a natural antagonist of BMP2, BMP4, and BMP7, in a conditional knockout mouse model induced expansion of a Barrett's-like neo-columnar epithelium from multi-lineage glands. Conversely, in this model specific inhibition of BMP2 and BMP4 led to the development of a neo-squamous lineage. In an ablation model, inhibition of BMP2 and BMP4 resulted in the regeneration of neo-squamous epithelium after the cryoablation of columnar epithelium at the squamocolumnar

junction. Through lineage tracing the generation of the neo-squamous mucosa was found to originate from K5+ progenitor squamous cells.

CONCLUSIONS: Here we demonstrate that specific inhibitors of BMP2 and BMP4 attenuate the development of Barrett's columnar epithelium, providing a novel potential strategy for the treatment of Barrett's esophagus and the prevention of esophageal adenocarcinoma. *(Cell Mol Gastroenterol Hepatol 2023;15:1199–1217; https://doi.org/10.1016/j.jcmgh.2023.01.003)*

Keywords: BMP2; BMP4; Llama-Derived Single-Domain Antibody; Targeted Therapy; Barrett's Esophagus; Preclinical Models.

Barrett's esophagus (BE) is an epithelial type of metaplasia that results from inflammatory signals caused by chronic duodeno-gastroesophageal reflux disease (DGERD).[1,2] BE patients require preventive measures to reduce reflux such as acid suppression medication, and in therapy resistant cases, fundoplication, a surgical procedure where the upper part of the stomach is attached to the lower esophagus, is performed to prevent acid reflux.[3,4] BE patients are also required to undergo periodic surveillance to detect and prevent chronic inflammation and reduce the risk of progression to dysplastic BE and esophageal adenocarcinoma (EAC).[3–5] Over several decades, the incidences of BE and EAC have been increasing. Because the majority of individuals with BE are not diagnosed, many EAC patients are detected with advanced disease stage and poor prognosis.[5,6] Throughout the past years, there has been an improvement of surgical and endoscopic treatment options for BE patients, such as endoscopic mucosal resection, endoscopic submucosal dissection, cryoablation, or radiofrequency ablation.[6–8] Nevertheless, patients undergoing these lines of treatments can still have residual buried Barrett's cells, which leads to recurrence of BE disease, making current surveillance and treatment challenging. Importantly, only a minority of BE patients (<10%), those who have progressed to dysplasia, are eligible for these relatively costly endoscopic approaches.[9] To develop more advanced and efficient targeted therapies, a greater understanding of the disease process at the molecular level is needed. However, achieving a greater understanding will require improved preclinical models so that the disease biology can be more closely studied, and novel therapies can be tested.

Bone morphogenetic proteins (BMPs) are members of the transforming growth factor-β (TGF- β) superfamily.[10] BMPs have essential roles in embryonic development and in the homeostasis of several organs and tissues including the homeostasis and differentiation of intestinal cell lineages.[11,12] The BMP subfamily is composed of more than 20 members and can be divided into different subgroups, eg, BMP2/4, BMP5/6/7/8a/8b, BMP9/10, and BMP 12/13/14, depending on their structure, amino acid sequence, and functions.[10] The embryonic development of the esophagus is regulated by BMP4 and by one of its natural inhibitors, noggin.[13] Noggin binds to the BMP2, BMP4, and, to a lesser extent, the BMP7 proteins, preventing them from binding to their receptors and activating downstream signaling pathways.[14,15] The normal adult esophagus is characterized by low levels of BMP2 and BMP4 and high levels of BMP7, especially within the upper basal layer; BMP7 is required for the physiological differentiation of the stratified squamous epithelium.[16,17] Sonic hedgehog (SHH) induces BMP4 expression, which leads to the activation of the BMP4-pSMAD pathway.[18] Up-regulation of the SHH mediated canonical BMP4-pSMAD pathway has been identified as a key determinant in the shift from normal squamous cells to the columnar and intestinal cells characteristic of Barrett's metaplasia.[16,19,20] Increased levels of BMP4 are seen in squamous mucosal biopsies after exposure to bile acids alone and in the setting of active inflammation caused by DGERD.[16,21] Importantly, in murine models with induced inflammation of the esophagus through bile reflux or overexpression of interleukin-1 beta or BMP4, activation of the BMP pathway leads to the proliferation of neo-columnar epithelium at the squamocolumnar junction (SCJ) in the stomach, resembling BE.[19,22] This highlights the important role of BMP4 in the development of BE.

On the basis of these studies, we hypothesize that specific targeting of members of the canonical BMP-pSMAD pathway could result in inhibition of Barrett's epithelium and thus represent an attractive molecular therapeutic option in the treatment of BE patients. Through a comprehensive pathway analysis in biopsies of human BE and squamous epithelium at the gene and protein expression level, we found that BMP2 and BMP4, but not other BMPs, are highly up-regulated in BE and found an overall high activity of the BMP canonical signaling. This suggested that selective inhibition of BMP2 and BMP4 could be sufficient to inhibit or repress BE development. To test this hypothesis, we developed different preclinical mouse models to test our recently generated BMP-specific llama-derived antibodies. These llama-derived anti-BMP2/4 antibodies have high specificity and effectivity for inhibition of BMP2/4.[23,24] We tested the effects of BMP inhibition in a novel in vivo organoid model, a conditional noggin knockout mouse model, and a cryoablation mouse model. In all 3 models, BMP2 and BMP4 inhibition decreased the number of Barrett/columnar cells, enhancing the growth of squamous cells. Using a lineage tracing strategy in the K5-cre-Tomato-GFP mouse model, we observed that the neo-squamous epithelium seems to originate from cytokeratin 5+ (K5+)

***Authors share co-first authorship.**

Abbreviations used in this paper: **BE, Barrett's esophagus; BMP, bone morphogenetic protein; DGERD, duodeno-gastroesophageal reflux disease; EAC, esophageal adenocarcinoma; GFP, green fluorescent protein; PCR, polymerase chain reaction; PPI, proton pump inhibitor; SCJ, squamouscolumnar junction; SHH, sonic hedgehog; SQ, squamous; TGF-β, transforming growth factor-beta.**

Most current article

2352-345X
https://doi.org/10.1016/j.jcmgh.2023.01.003

progenitor cells. In sum, we show that selective inhibition of BMP2 and BMP4 effectively suppresses Barrett's epithelium and enhances re-epithelialization by squamous cells. We propose that BMP2 and BMP4 inhibition using anti-BMP2/4 inhibitors represents an attractive molecular therapy for the future treatment of BE.

Results

Gene Expression of SHH-TGF-β/BMP Signaling in Esophageal Human Squamous and Barrett's Biopsies

Previous studies have reported higher *BMP4* mRNA levels and up-regulation of BMP4 protein levels in different esophageal cell lines as well as in BE tissue biopsies when compared with normal squamous epithelium.[16,21,25] These reports might indicate a role of BMP4 in the differentiation of columnar cells. Unfortunately, a thorough examination of the expression levels of other BMPs and associated signaling pathways in BE biopsies is lacking. This is an important issue to study, because selective targeting of one member might not lead to sufficient inhibition of BMP signaling because of the similar and overlapping functions of these molecules.

Here, we performed a comprehensive analysis of the RNA expression of SHH–TGF-β/BMP signaling pathways in Barrett's mucosal biopsies and compared that with normal squamous mucosa biopsies. Hierarchical clustering of genes expressed within the SHH–TGF-β/BMP pathways showed an overall up-regulation of *SHH–TGF-β/BMP* signaling mRNA levels in Barrett's biopsies compared with normal squamous mucosa (Figure 1*A*). Differential expression analysis, followed by Ingenuity Pathway analyses, showed the up-regulation of BMP pathway signaling in the BE biopsies is through increased expression of *BMP2* and *BMP4,* whereas *BMP7* seems to be down-regulated in the BE biopsies and up-regulated in squamous mucosa (Figure 1*B*).

Immunohistochemistry of Barrett's biopsies confirmed the increased protein expression of BMP2 and BMP4 and their downstream targets pSMAD1/5/8, ID1, and ID2 (Figure 1*C*). Data were further validated by Western blot, where we confirmed the higher protein expression of BMP2, BMP4, BMP5, and BMP6 in human Barrett's biopsies (Figure 2*C*).

To visualize the effect of bile acids, the putative risk factor for BE, different mouse and human cell lines were exposed to conjugated bile acids.[28] In mouse primary esophageal keratinocytes and human squamous EPC2-hTERT cell lines, bile acids significantly promoted the expression of BMP7 after 24 hours and 48 hours of bile acids exposure. BMP2, BMP4, and SHH were also up-regulated, but not significantly, in the mouse primary esophageal keratinocytes. Bile acids also induced BMP2 up-regulation and significant up-regulation of BMP4 at 8 hours and 24 hours and BMP7 and SHH after 48 hours of bile acid exposure in the human CP-A BE cell line (Figure 2*D*).

In sum, BMP2 and BMP4 are BMPs that are most highly expressed in BE, when compared with squamous tissue, and therefore represent potential therapeutic targets in comparison with the other BMPs. These results were further validated in a different cohort of BE patients in a Gene Expression Omnibus dataset (Wang 2013, accession number GSE26886; Figure 2*A*).[29]

Effects of BMP4 and BMP2/4 Inhibition in an in Vivo Organoid Model of Human Barrett's Esophagus Biopsies

Most of the currently available BMP inhibitors and antagonists are not selective for targeting single-family members such as BMP2 or BMP4. Previously, we isolated highly specific llama-derived antigen-binding fragments, which selectively inhibit BMP4 (anti-BMP4) or BMP2 and 4 (anti-BMP2/4).[23,24] We hypothesized that inhibition of BMP2 and BMP4 with our llama-derived antibody might be sufficient to inhibit the development of Barrett's epithelium. To test this hypothesis, we developed a novel in vivo organoid model by intramuscular implantation of endoscopically obtained human BE or squamous biopsies in NSG mice. This innovative animal model allows the growth of human biopsies to an organoid structure that resembles either squamous or BE columnar epithelium and permits testing the effects of therapies by intraperitoneal injection (Figure 3*A–D*). The humanized in vivo Barrett's and squamous organoids expressed the human mitochondrial antigen, which confirmed the human origin of the generated in vivo organoid (data not shown). The squamous biopsies and corresponding in vivo organoids showed similar multilayered lining of Alcian blue$^-$, CDX2$^-$, p63+, and K5+ squamous cells with a region resembling squamous papillae (Figure 3*C*). The Barrett's biopsies and corresponding in vivo organoids were lined with a secretory CDX2+ columnar epithelial layer and containing Alcian blue+ mucus-producing goblet cells (Figure 3*D*). At the basal side of the mucous cells, a few p63+, K5+ squamous cells could be observed.

Subsequently, BE biopsies were grown for 8–12 weeks, while treated with llama-derived anti-BMP4 and anti-BMP2/4 antibodies. NSG mice were treated with anti-BMP4, anti-BMP2/4, or saline, starting 1 week after intramuscular implantation of the human Barrett's biopsies (Figure 3*E*). Treatment with anti-BMP4 at the dose tested gave rise to an organoid with a mixed epithelial layer characterized by a multilayered squamous epithelium with p63+, K5+ cells and a reduced number of mucus producing cells (Figure 3*F*). Treatment with anti-BMP2/4 at the dose tested resulted in p63+/K5+ multilayered epithelium, weakly expressing K19 but with Involucrin+ and Sox2 expressing cells (Figure 3*F* and Figure 4). Mucus producing Alcian blue+ and CDX2+ cells were absent (Figure 3*F*). The numbers of Ki67+ proliferative cells in both saline-treated mice and anti-BMP2/4–treated mice were reduced in the Barrett's organoids treated with anti-BMP2/4, when compared with the original biopsies (Figure 4). Interestingly, we observed that a

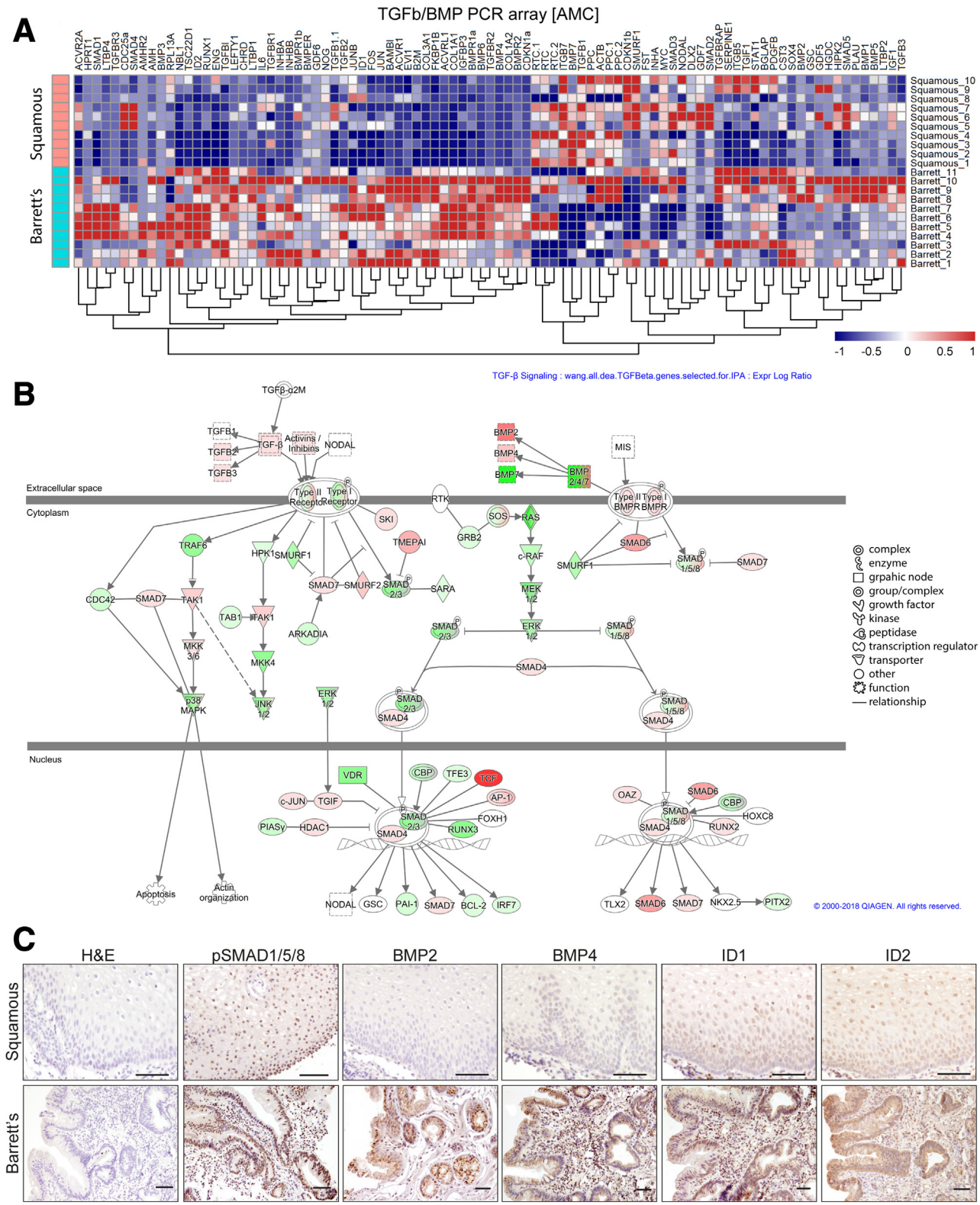

Figure 1. Gene expression of SHH-TGF-β/BMP signaling in esophageal human squamous and Barrett's biopsies. (*A*) Clustering of gene expression values of TGF-β/BMP pathway genes in patient-derived biopsies of BE and normal esophageal squamous mucosa (SQ). Gene-clustered heatmap was drawn for quantitative PCR data using the heatmap package, after log transformation and calculation of z-scores for all samples per gene. (*B*) Ingenuity Pathway Analysis of TGF-β/BMP signaling in Barrett's esophagus compared with normal squamous tissue.[26] (*C*) Representative immunohistochemistry for BMP2 and BMP4 and their downstream targets pSMAD1/5/8, ID1, and ID2 in normal squamous and Barrett's biopsies. Hematoxylin was used as a counterstain. (Scale bars: 100 μm).

population of remnant p63+ and K5+ squamous cells were also observed in the original Barrett's biopsy that corresponded with the treated Barrett's implant (Figure 3*D* and Figure 5*B*).

To determine the possible side effects of BMP2/4 inhibition in other organs, we analyzed the histology of the colons from all mice, because BMP2 and BMP4 have active roles in this tissue where BMP2/4 have important function. We observed that BMP2/4 inhibition also resulted in a transient loss of goblet cells in the colon, which recovered 4 weeks after the end of treatment (Figure 6). Also, all mice presented normal weights, stools, and behavior during the treatments.

Thus, in a novel organoid model that sustains Barrett's and squamous epithelia, inhibition of only BMP4 at the dose tested was not enough to reduce the BE phenotype. Inhibition of both BMP2 and BMP4 was required for a selective reduction of all Barrett's columnar and mucus producing goblet cells and favored the proliferation and establishment of squamous epithelium.

Effects of BMP2/4 Inhibition on Neo-Columnar Epithelium Development in a Conditional Noggin Knockout Barrett's Model

Although the in vivo human BE organoid model allowed us to observe the effect of BMP2/4 inhibition in human BE tissue, we were not able to observe the effect of BMP2 and BMP4 inhibition during the development of the neo-columnar BE epithelium.

The use of tamoxifen-inducible noggin knockout (noggin$^{-/-}$) mice, where the BMP signaling cascade is up-regulated, allows us to study the impact of BMP2/4 inhibition on the development of neo-columnar epithelium.[30] Noggin knockdown in mice is an embryonically lethal phenotype; however, analysis of the fetal tissue showed aberrant columnar cells lining the esophagus.[31] Therefore, we generated a conditional noggin knockout mouse model by crossing Rosa26-Cre/ERT2 mice with loxP [Noggin] loxP mice. After tamoxifen injection, this tamoxifen-inducible noggin$^{-/-}$ model develops columnar metaplasia at the SCJ and is a representative model of the development of columnar metaplasia (Figure 7*A*).

As expected, tamoxifen injection at 8 weeks resulted in the absence of noggin in the esophagus, forestomach, stomach body, antrum, intestine, and colon in adult mice (Figure 8*A*). After 24 weeks of tamoxifen injection, in line with previous observations,[31] the tamoxifen-inducible noggin$^{-/-}$ mice maintained expression of BMP4 and pSMAD1/5/8 comparable with the wild-type controls (Figure 8*B*). Also, there were no significant differences in morphology and histology of the esophagus, intestine, and colon (Figure 8*C*). However, 4 weeks after the deletion of noggin, we observed expanded multi-lineage glands at the SCJ in the stomach, characterized by abundant neo-columnar epithelium resembling Barrett's columnar metaplasia (Figure 7*A*).[19,32] To investigate whether BMP2/4 inhibition can inhibit the expansion of the neo-columnar epithelium from the multi-lineage glands and at the same time enhance the expansion toward neo-squamous epithelium, the tamoxifen-inducible noggin$^{-/-}$ mice were treated with anti-BMP2/4 (Figure 7*B*). Eight weeks of systemic treatment with anti-BMP2/4 resulted in decreased BMP canonical signaling in the mice stomach, as can be observed by a reduction in pSMAD1/5/8 expression (Figure 7*C*). Inhibition of BMP2 and BMP4 resulted in increased proliferative activity of the squamous layer, which may originate from the outer layer of the multi-lineage glands. In addition, there was an expansion of the multilayered neo-squamous epithelium and the development of papillae-like structures (Figure 7*B*).

Thus, the conditional deletion of noggin resulted in the development of a Barrett's-like neo-columnar epithelium at the SCJ in the stomach of mice. The inhibition of BMP2 and BMP4 inhibited the neo-columnar lineage and enhanced the development of a neo-squamous epithelium. We hypothesize that both the neo-columnar and neo-squamous lineages are derived from the multi-lineage glands residing at the SCJ in mice; however, this observation needs further investigation in lineage tracing experiments.

Anti-BMP2/4 Treatment and Lineage Tracing of K5+ Progenitor Cells in a Cryoablation Model of Premalignant Columnar Lesions

To further investigate the potential of the llama-derived anti-BMP2/4 antibodies and complement the previous models with regard to translatability, we explored the translational effect of our antibodies using a unique cryoablation in vivo model. The cryoablation model consists of the ablation of the columnar mucosa at the SCJ of the stomach of mice through local application of liquid N_2O to test the potential of different therapies for prevention of neo-squamous epithelia developed at the SCJ in mice stomach. This cryoablation model resembles a clinical therapeutic setup, which not only can be valuable to test potential adjuvant therapies but also is a valuable model to investigate the origin of the neo-squamous cells.

In wild-type CB6F1/Crl mice, cryoablation of the columnar mucosa in the forestomach just distal to the SCJ resulted in the regeneration of normal stomach columnar epithelium and restored architecture of the crypts after 21 days (Figure 9*A*–*C*). In cryoablated mice and treated with the anti-BMP2/4 for 21 days (500 μg/mL daily), the ablated columnar stomach epithelium was replaced by a multilayered K5+ and p63+ neo-squamous epithelium that poorly expresses the columnar marker K19 (Figure 9*D*).

The repopulation of the esophageal mucosa at the SCJ was further investigated by using a K5–green fluorescent protein (GFP) lineage tracing mouse model. Using K5-Cre/ERT2 mice crossed with Rosa26-Tomato-loxP [stop] loxP-GFP mice, injection of tamoxifen activated the GFP reporter gene in K5+ cells, permanently marking these cells and their progeny as they repopulate the mucosa

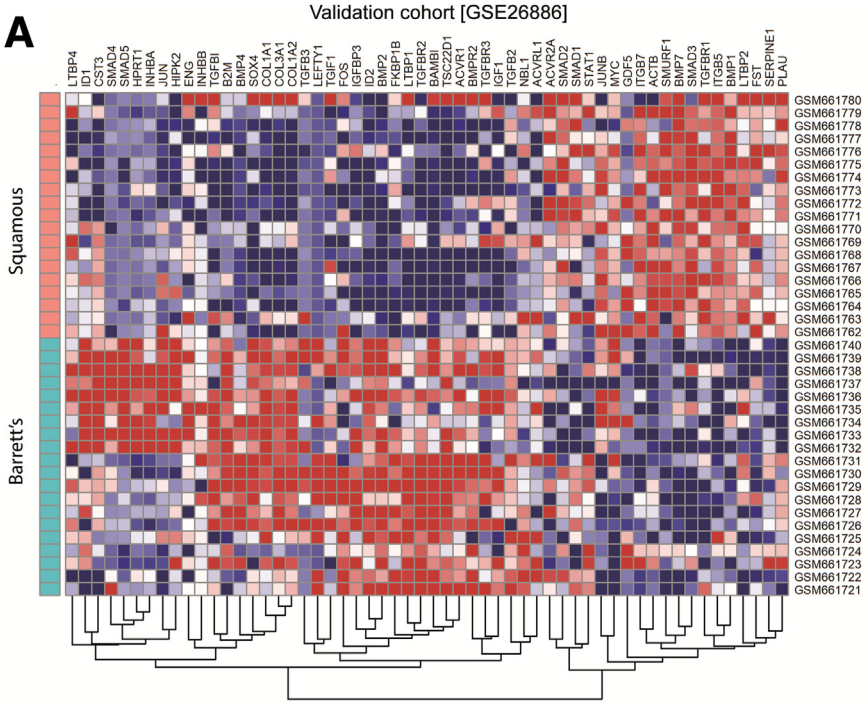

B

	SHH/WNT PCR array [AMC]		Validation cohort [Wang 2013]	
	log2FC	p value	log2FC	p value
HHIP	6,39	0	3,87	0
SHH	6,29	0	2,79	0
BMP5	6,11	0,01	NA	NA
IHH	4,87	0	2,37	0
FGF9	4,38	0	2,7	0
ZIC2	4,26	0,02	1,54	0,03
BMP2	3,64	0	4,33	0
BMP4	3,57	0	1,89	0
PTCH1	2,98	0	3,13	0
BMP6	2,5	0	NA	NA
PRKACB	2,25	0	4,11	0
GLI1	1,97	0,03	NA	NA
RAB23	1,95	0,03	1,7	0
PTCH2	1,51	0,04	NA	NA
CRIM1	1,48	0	1,14	0
DHH	1,44	0,04	NA	NA
CTNNB1	1,39	0	0,73	0
IFT52	0,94	0,02	-0,17	0,35
NUMB	0,93	0	NA	NA
SIAH1	0,88	0	-0,31	0,1
C18orf8	0,84	0	0,17	0,5
STK36	0,8	0	0,56	0,01
CSNK1D	0,67	0,04	-1,3	0
CSNK1G2	0,63	0,05	-0,6	0
OTX2	-0,61	0,04	NA	NA
CSNK1A1L	-1,06	0,01	NA	NA
PRKX	-1,14	0,03	-3,42	0
MTSS1	-1,28	0,05	-2,01	0
WNT4	-1,57	0,04	-4,95	0
FGFR3	-1,7	0,03	-3,86	0
BMP7	-1,75	0,02	-3,16	0
WNT5A	-2,15	0,01	-2,45	0
WNT10A	-2,7	0,03	-0,6	0,1
WNT7B	-5,53	0,03	NA	NA
FOXE1	-6,2	0,02	-4,75	0

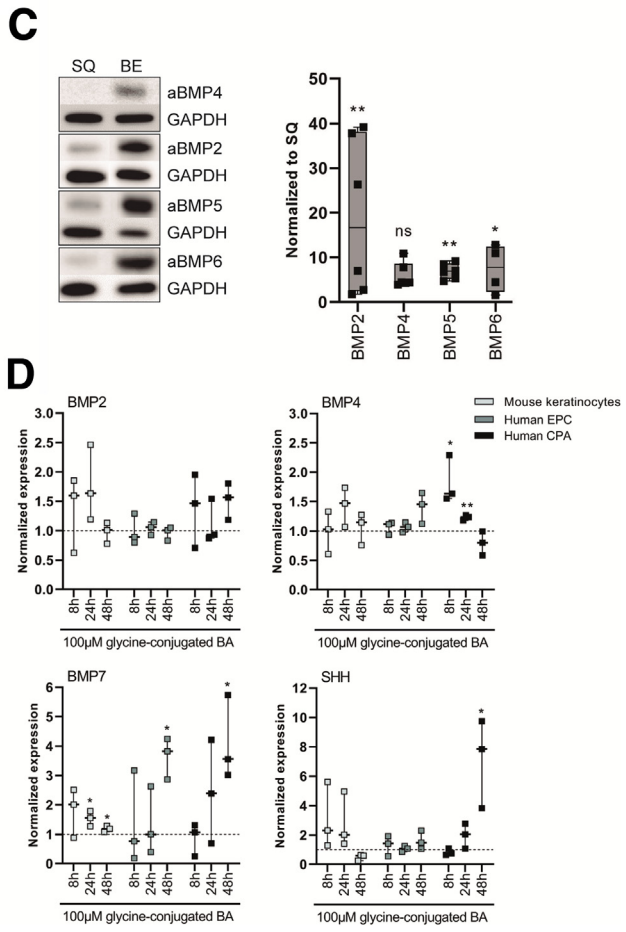

(Figure 9*E*). After the cryoablation of the columnar epithelium, the re-epithelization of the stomach in the K5-GFP mice was comparable with that of the wild-type CB6F1/Crl mice (Figure 9*D* and *F*). The SCJ in mice can be identified by the formation of the characteristic SCJ loop, which is identified in Figure 9 with asterisk (*). Treatment of the K5-GFP mice with anti-BMP2/4 for 21 days resulted in the appearance of a GFP+ neo-squamous epithelium replacing the ablated columnar epithelium (Figure 9*F*). Local treatment of noggin, previously shown by Correia et al,[33] also enhanced the development of neo-squamous epithelium in the ablated area. The GFP expression indicates the neo-squamous cells originate from K5+ progenitor cells (Figure 9*F*).

Discussion

Metaplastic changes are associated with up-regulation of signals and pathways that are involved in embryonic development.[11,12] SHH, TGF-β, and the BMP signaling pathways are activated during the earliest stages of tissue and organ development.[34] BMPs are highly homologous molecules that signal via their receptors BMPR I and II. Because of interactions with diverse transcription and regulatory factors and through non-canonical signaling, their effects are highly pleiotropic.[19]

Here we performed a thorough gene expression analysis and validation of the SHH–TGF-β/BMP signaling pathway in human biopsies, and we found that apart from BMP4, BMP2 was also highly expressed in BE. Therefore, both BMP2 and BMP4 seemed to be attractive therapeutic targets within the BMP signaling cascade for the treatment of BE.[16,19] In contrast, there was high BMP7 and TGF-β activity in the squamous mucosa, which is in line with the study by Jiang et al.[17] BMP2 and BMP4 are structurally similar with comparable functions and are categorized to the same subgroup of the BMP superfamily.[10] Thus, it is not surprising to observe that both BMP2 and BMP4 interact for a common function. Currently, most inhibitors of BMP2 and BMP4 and including small molecules inhibitors not only inhibit BMP2 and BMP4 but also other BMPs. Because of the homeostatic role of the different BMPs in the different organs, unselective inhibition of BMP signal can lead to detrimental effects. In our study we only wanted to target BMP2 and/or BMP4 but not BMP7, which is critical for the homeostasis of squamous epithelium. In our group, we developed highly specific and effective llama-derived antibodies against BMP4 and BMP2/4. Our inhibitors are proven to be more specific when compared with commercially available inhibitors and natural antagonists or small molecule inhibitors.[23,24] On the basis of the gene expression analysis, we hypothesized that using the llama-derived anti-BMP2/4 antibodies would be most optimal to provide inhibition of BE development, whereas inhibition of BMP4 alone would not be sufficient. This hypothesis was confirmed in our in vivo organoid model of human BE biopsies, where we found that inhibition of both BMP2 and BMP4 led to a decrease in the proliferation of columnar cells, enhancing the development of a neo-squamous epithelium. At the dosage tested, the same result was not obtained when only BMP4 was inhibited. This indicates that together BMP2 and BMP4 may have a stronger and overlapping role in the development of BE. As previously shown in different cell lines by Barros et al,[35] BMP2 and BMP4 are closely related and regulate CDX2 expression and promote intestinal differentiation in other columnar tissues.

Inhibition of both BMP2 and BMP4 also prevented the formation of a human in vivo organoid with Barrett's type of columnar cells by selectively reducing columnar and goblet cells and prioritizing the proliferation and establishment of squamous epithelium. This was most likely possible because the function of BMP7, which is essential for squamous differentiation, was left intact.[17] We believe that the remnant K5+, p63+ squamous progenitor cells observed in the corresponding Barrett's biopsies gave rise to the neo-squamous epithelium. Earlier reports have described the presence of p63+ cells in submucosal glands in BE and also in the proliferative compartment of Barrett's non-neoplastic epithelium.[36,37]

Inhibition of BMP2 and BMP4 has been shown to lead to repression of existing BE in our organoid model; however, it does not tell us whether it can inhibit the development of BE. To further test this possibility, we used our llama-derived anti-BMP2/4 antibodies in a tamoxifen-inducible noggin$^{-/-}$ mouse model because noggin is a natural antagonist of the function of different BMPs including BMP2, BMP4, and BMP7.[38] Tamoxifen-inducible noggin$^{-/-}$ mice present enhanced BMP activity and develop columnar metaplasia resembling Barrett's mucosa, where the neo-columnar epithelium seems to ascend from multi-lineage glands that reside at the SCJ.

Figure 2. (***See previous page***). **(*A*) Clustering of RNA expression in biopsies from Barrett's and squamous tissue and from a validation cohort (Wang 2013, GSE26886).**[27] Gene-clustered heatmap was drawn for quantitative PCR data using the heatmap package, after log transformation and calculation of z-scores for all samples per gene. (*B*) Quantitative PCR of SHH/WNT pathway genes in biopsies from Barrett's and squamous tissue from AMC patients (*left*) and from a validation cohort (*right*) (Wang 2013, GSE26886).[27] Genes significantly differentially expressed in Barrett's compared with squamous in the AMC cohort ($P < .05$). (*C*) Western blot analysis of BMP2, BMP4, BMP5, and BMP6 in Barrett patient's (BE) biopsies (*left panel*). Levels of BMPs in Barrett's biopsies were quantified and normalized to squamous tissue (SQ). Data are represented in *box and whiskers plot* of at least 4 independent experiments. (*D*) BMP2, BMP4, BMP7, and SHH mRNA levels by quantitative PCR in mouse esophageal keratinocytes, human normal squamous esophageal EPC2-hTERT, and Barrett's CP-A cells, after treatment with glycine-conjugated bile acid (100 μmol/L) for 8, 24, or 48 hours. Data are represented in *box and whiskers plots* as mean of at least 3 independent experiments. *$P < .05$, **$P < .01$, ***$P < .001$. ns: not significant.

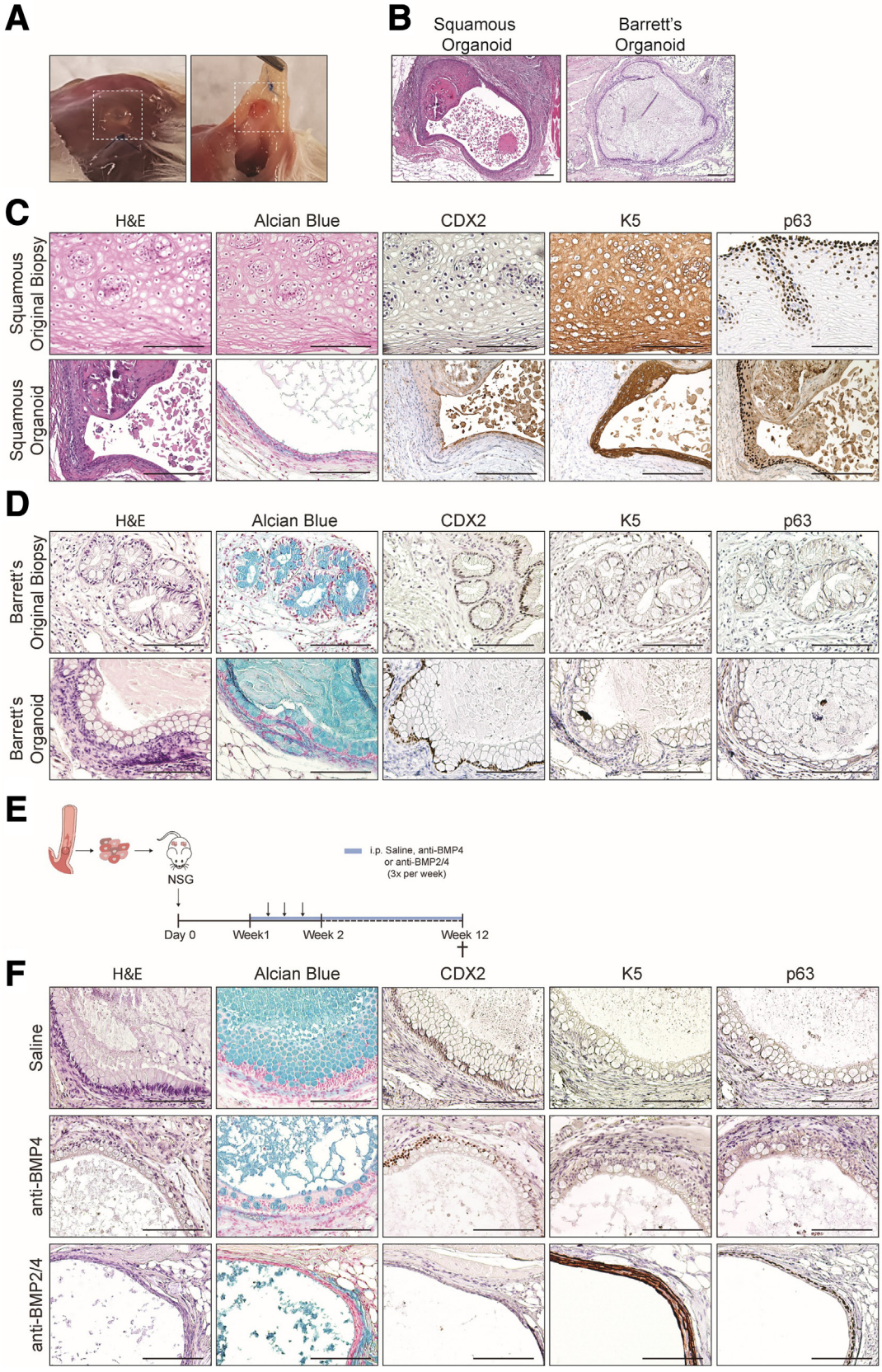

Figure 3. Effects of BMP4 and BMP2/4 inhibition in in vivo organoid model of human BE biopsies. (*A*) Dissection of in vivo organoid from the dorsal musculature of NSG mouse. (*B*) H&E staining of complete squamous and Barrett's in vivo organoid. (*C*) H&E, Alcian blue staining, and immunohistochemistry (IHC) for CDX2, K5, and p63 of a squamous biopsy and corresponding organoid and (*D*) of Barrett's biopsy and corresponding organoid. (*E*) Experimental setup of intramuscular implantation of human biopsies to obtain in vivo organoids and treatment schemes with saline and the anti-BMP inhibitors. (*F*) H&E, Alcian blue staining, and IHC of CDX2, K5, and p63 of Barrett's in vivo organoids treated with saline, anti-BMP4, or anti-BMP2/4. Hematoxylin was used as a counterstain. (Scale bar: 200 μm).

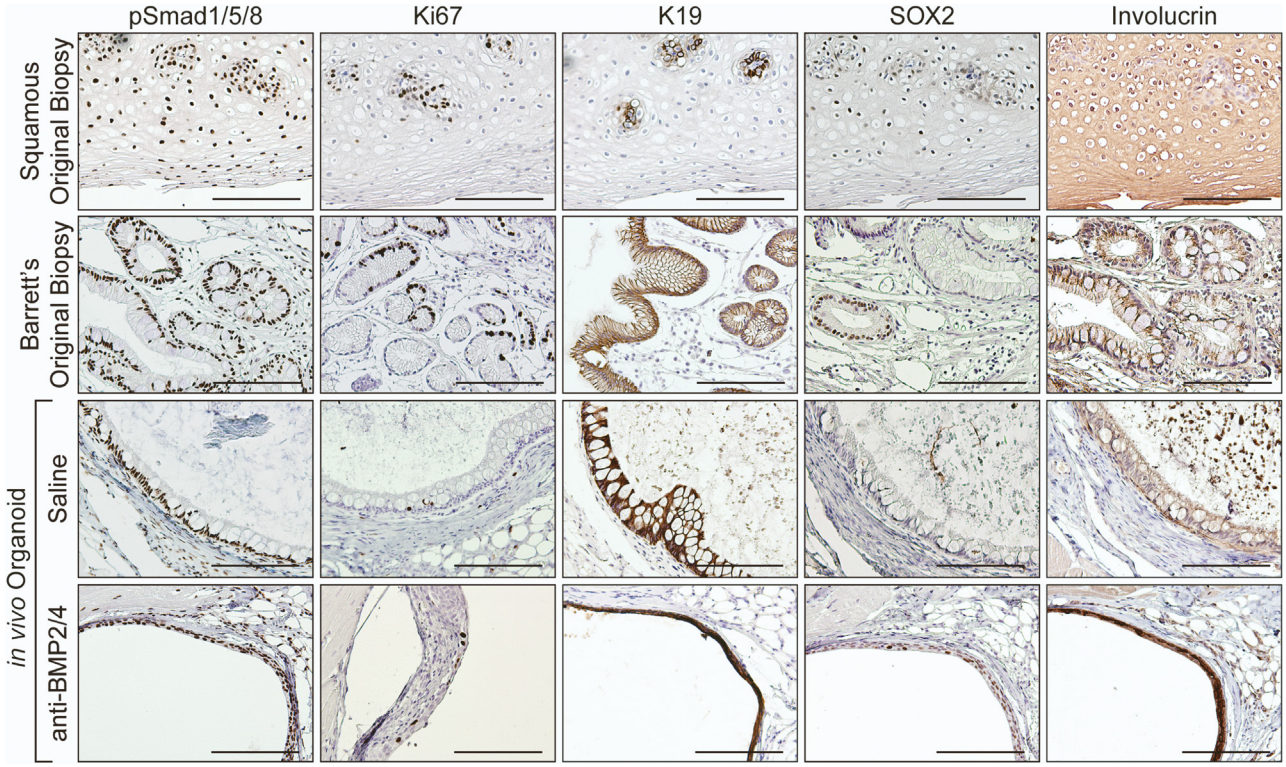

Figure 4. Immunohistochemistry (IHC) staining of squamous and Barrett's biopsies in comparison with the corresponding in vivo Barrett's organoid treated with saline or anti-BMP2/4 antibody. IHC staining for pSMAD1/5/8, Ki67, K19, SOX2, and Involucrin. Hematoxylin was used as a counterstain. (Scale bar: 100 μm).

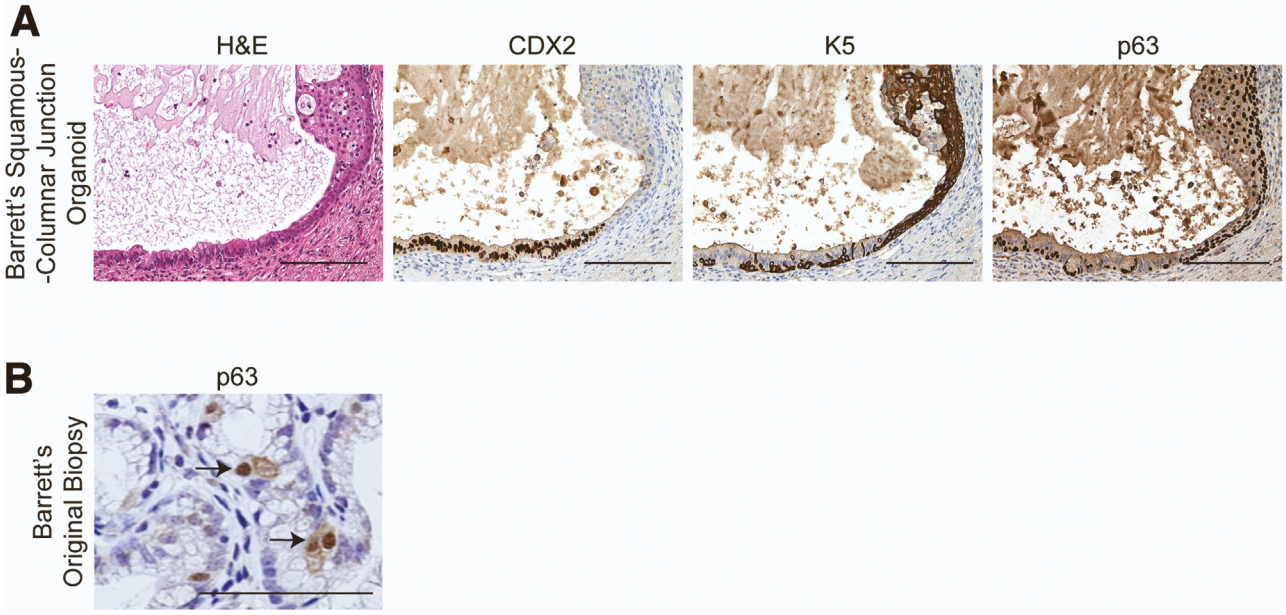

Figure 5. (*A*) H&E and IHC for CDX2, p63, and K5 of in vivo organoid obtained from biopsy taken at the SCJ from a Barrett's patient. (*B*) IHC staining of p63+ remnant cells (*arrows*) in a BE biopsy. Hematoxylin is used as a counterstain (scale bar: 200 μm). SCJ, squamocolumnar junction.

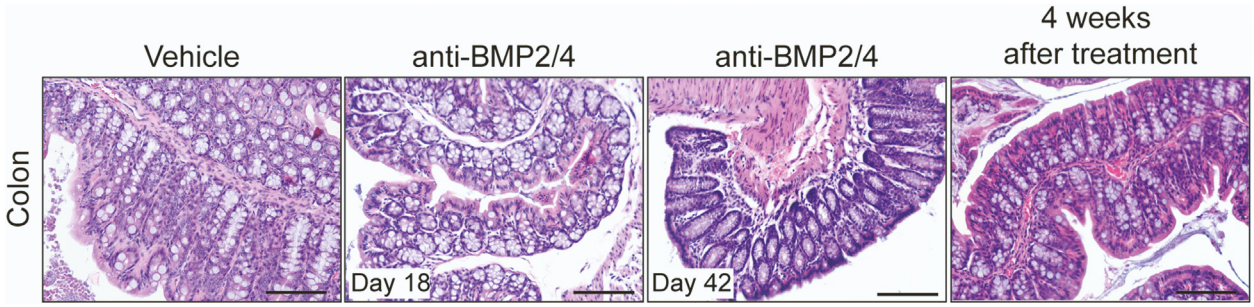

Figure 6. Effect of anti-BMP2/4 antibody treatment on colon of wild-type mice. H&E staining of the colon in mice at different time points of anti-BMP4 and anti-BMP2/4 antibodies treatment. (Scale bar: 200 μm).

This observation is in line with the model developed by Jiang et al.[17] However, further experiments such as lineage tracing experiments in tamoxifen-inducible noggin$^{-/-}$ mice are required to prove this observation.[32] Consistent with our findings in our in vivo organoid model, inhibition of BMP2 and BMP4 in the noggin knockout model inhibited the neo-columnar epithelium and enhanced the development of a neo-squamous epithelium.

The cryoablation model, where the columnar and squamous mucosa at the SCJ of the stomach of mice is ablated, allowed us to further investigate the effect of BMP2/4 inhibition on the homeostasis of normal columnar tissue and to understand the origin of the neo-squamous epithelium at the SCJ. By implementing the ablation method in a lineage tracing model of K5+ cells, we could further investigate the origin of the neo-squamous cells. After ablation, anti-BMP2/4 treatment inhibited the regeneration of normal columnar stomach epithelium in our K5-GFP lineage tracing model. The ablated epithelium was replaced by neo-squamous epithelium, which originated from K5+ squamous progenitor cells, visualized by lineage-tagged GFP+ cells in the K5-GFP mouse model. In this model we presume that the K5, p63+ neo-squamous cells originated from the outer layer of the submucosal glands, which is in accordance with the recent article by Jiang et al.[32]

In summary, we found that BMP2 and BMP4 signaling is highly active in BE, whereas in normal squamous mucosa TGF-β pathways and BMP7 are higher. We demonstrated that specific inhibition of BMP2 and BMP4 effectively inhibited the regeneration of human Barrett cells in an organoid model and in a neo-columnar epithelium of transgenic mice resembling BE and cryoablation model. Because our novel inhibitor is highly specific for BMP2 and BMP4 and has no effect on BMP7, the regeneration of normal stratified squamous epithelium was not affected or even favored in our different models. This is a targeted therapy that can potentially be applied for treatment of a columnar metaplastic lesion. In the future such therapy might be a good option to be implemented as a complementary clinical approach for the treatment of BE together with ablative therapies or even as a pre- or post-ablation approach. If successful, this could prevent cancer progression and eventually reduce the burden of costly BE surveillance programs.

Materials and Methods

Ethics

Use of all human patient material was approved by the institutional Medical Ethical Committee of the Amsterdam UMC, Academic Medical Centre Amsterdam (AMC), MEC 01/228, and the study was conducted according to our institution's ethical guidelines and the Helsinki declaration. All patients gave informed consent to participate in the study before sample collection.

Samples were collected during the routine endoscopic surveillance program at the Gastroenterology and Hepatology Department of the AMC. All patients were on long-term proton pump inhibitor (PPI) therapy. After a confirmed diagnosis of intestinal metaplasia without dysplasia by endoscopy and histology, samples were used in our study.

All animal research was conducted under protocols approved by the Animal Experimental Committee of the AMC in compliance with the Animal Welfare Body (IvD) under the protocol numbers LEX159 and LEX194. Animals were kept in the Animal Research Institute of the AMC (ARIA), and experiments were performed under ARIA standard operating procedures.

In Vivo Organoid Model of Human Barrett's Esophagus Biopsies

NOD-scid IL-2 receptor gamma chain knockout (NSG) mice were purchased from The Jackson Laboratory and bred in house at the Animal Research Institute of the AMC. All mice were maintained in specific pathogen-free conditions, given autoclaved standard pellet feed and water ad libitum, and housed in ventilated racks. Fresh samples were collected endoscopically from the squamous epithelium and Barrett's segment of 4 different patients. All 4 patients had non-dysplastic Barrett and no active reflux on the endoscopy day. All patients used PPIs, and matching biopsies (taken side by side) or a piece of the implanted biopsies were checked by histopathology to confirm the presence of intestinal type of BE with no dysplasia.

Samples were placed in cold phosphate-buffered saline solution without $MgCl_2$ and $CaCl_2$, supplemented with 200 U/mL penicillin and 200 μg/mL streptomycin (Thermo Fisher Scientific), and kept on ice. Each biopsy was inspected under the microscope. Biopsies were cleaned from any blood remaining and confirmed the presence or absence of inflamed tissue and for the presence or absence of BE. Biopsies were divided into approximately 1- to 2-mm^3-sized pieces, and any necrotic areas and blood clots were discarded. Representative samples were fixed in 10% buffered formalin for histologic evaluation, and the remaining pieces for implantation were placed in Matrigel (Corning) and kept on ice until implantation. All biopsies were implanted within 2 hours of collection. Mice were anesthetized via an intraperitoneal injection of ketamine (100 mg/mL; Sigma-Aldrich) and xylazine (20 mg/mL; Sigma-Aldrich) solution. After weighing, mice were injected with 10 μL of the anesthetic solution per gram of body weight. The dorsum of each mouse was shaved and prepared with a betadine solution. Under aseptic conditions, a 15-mm midline incision was made immediately caudal to the dorsal hump at the level of the renal angle. Using blunt dissection, a skin flap was raised, and the skin was retracted laterally to expose the implantation site. A superficial stay suture was placed in the dorsal musculature immediately caudal to the lowest rib using a 4/0 braided absorbable suture. Then, an intramuscular pocket was created using a combination of sharp and blunt dissection until it was just large enough to accommodate the Barrett's biopsy. The Barrett's biopsy was then coated in Matrigel and placed in the intramuscular pocket before suture closing. One or 2 separate transplantation sites were used per mouse. A 4/0 non-absorbable suture was used to mark the site of implantation. The skin was closed using 3/0 braided absorbable suture. Implants were cultured for a maximum period of 12 weeks to form the in vivo organoid structures. Commencing 1 week after implantation and continuing for a total of 12 weeks, mice were treated with saline (control group), llama-derived anti-BMP4 or anti-BMP2/4 antibodies (100 μg/mL, 3 $\times$/week; treatment group) via intraperitoneal injections.[23] A total of 24 NSG mice were used in the treatment study, of which 21 could be analyzed: saline (n = 8), anti-BMP4 (n = 3), and anti-BMP2/4 (n = 10). Mice were treated for 12 weeks, and during this period mice were closely monitored for any sign of discomfort and/or stress throughout the experiment. NSG mice (N = 3) were not used in analysis of this experiment because the treatment was shorter than 4 weeks. At the end of the 12-week treatment period mice were culled using CO_2 inhalation. Immediately after culling, mice were shaved, and their skin was prepared. After identifying the non-absorbable marking suture, the muscle was incised around the site of xenograft, leaving a 2-mm-wide margin. After this, the muscle was retracted medially, and the in vivo organoid was harvested. Samples were fixed in 10% buffered formalin to be assessed both histologically and immunohistochemically.

Noggin Knockout (Noggin$^{-/-}$) Mouse Model

Nogtm1.1Rmh/J mice (Jackson Laboratory) were crossed with Rosa26-cre/ERT2 mice (Jackson Laboratory). Tamoxifen (1 mg, intraperitoneally; Sigma-Aldrich) was administered for 3 consecutive days to delete noggin in all cells expressing Rosa26-cre/ERT2. Stomach tissues were formalin-fixed and paraffin-embedded for H&E staining and for immunohistochemistry. A total of 32 noggin$^{-/-}$ mice treated with saline (n = 16) or anti-BMP2/4 (n = 16; daily, 100 μg/mL) and 32 wild-type controls treated with saline (n = 16) or anti-BMP2/4 (n = 16; daily, 100 μg/mL) were used.

Cryoablation Mouse Model of Premalignant Columnar Lesions

Cryoablation procedure was performed according to Correia et al.[33] In brief, CB6F1/Crl mice were purchased from Charles River Laboratories and housed in the ARIA. A total of 36 mice were included for the original experiments. Experiments were performed using 8- to 10-week-old male mice, with an initial weight above 20 grams. Before and after the procedure, animals received liquid food for 3 days. Afterwards, normal pellet food and tap water were available ad libitum. Because of procedural animal loss and reaching humane endpoints, 20 mice could be analyzed after 3 (n = 2), 7 (n = 6), 14 (n = 6), or 21 days (n = 6). Mice were subjected to inhalation of 2% isoflurane for induction and maintenance of anesthesia. The animals were gently fixed to a heating pad (37°C), and after weighing, the abdomen was shaved and cleaned with betadine solution. A single injection of painkiller (5 mg/kg Melovem; Dopharma) was administered subcutaneously. A 1.5- to 2-cm midline laparotomy was then made. With the help of atraumatic forceps, the stomach was exteriorized. A small gastrostomy was then made along the anterior border of the stomach and crossing the SCJ. Gastric contents were emptied as much as possible using atraumatic forceps and cotton swaps. Using a cryopen (Cryoalfa LUX), liquid nitrous oxide (N_2O) was applied to the posterior wall of the stomach at the SCJ to ablate the epithelium. Liquid N_2O was applied twice in the same location for 10 seconds each time. The stomach was closed with continuous stitches using an 8/0 non-absorbable suture. The sutured stomach was placed back inside the peritoneal cavity, and the abdominal wall and skin were closed separately using a 5/0 vicryl absorbable suture. Postoperatively and after recovering from anesthesia, mice received liquid food for 3 consecutive days; on the third day they had both liquid and normal pellet food available. Antibiotic water (400 g/mL Baytril 2.5%; Bayer) was also present for the first 5 days after surgery. Afterwards, autoclaved tap water was available ad libitum. The animal cages were kept on a warming blanket for the first 24 postoperative hours. Animals were euthanized if they displayed signs of suffering, such as >15% weight loss after surgery. Throughout the experiment, mice received daily oral gavage of omeprazole (400 mol/kg; Teva Pharmaceuticals) and intraperitoneal injection of either saline (control

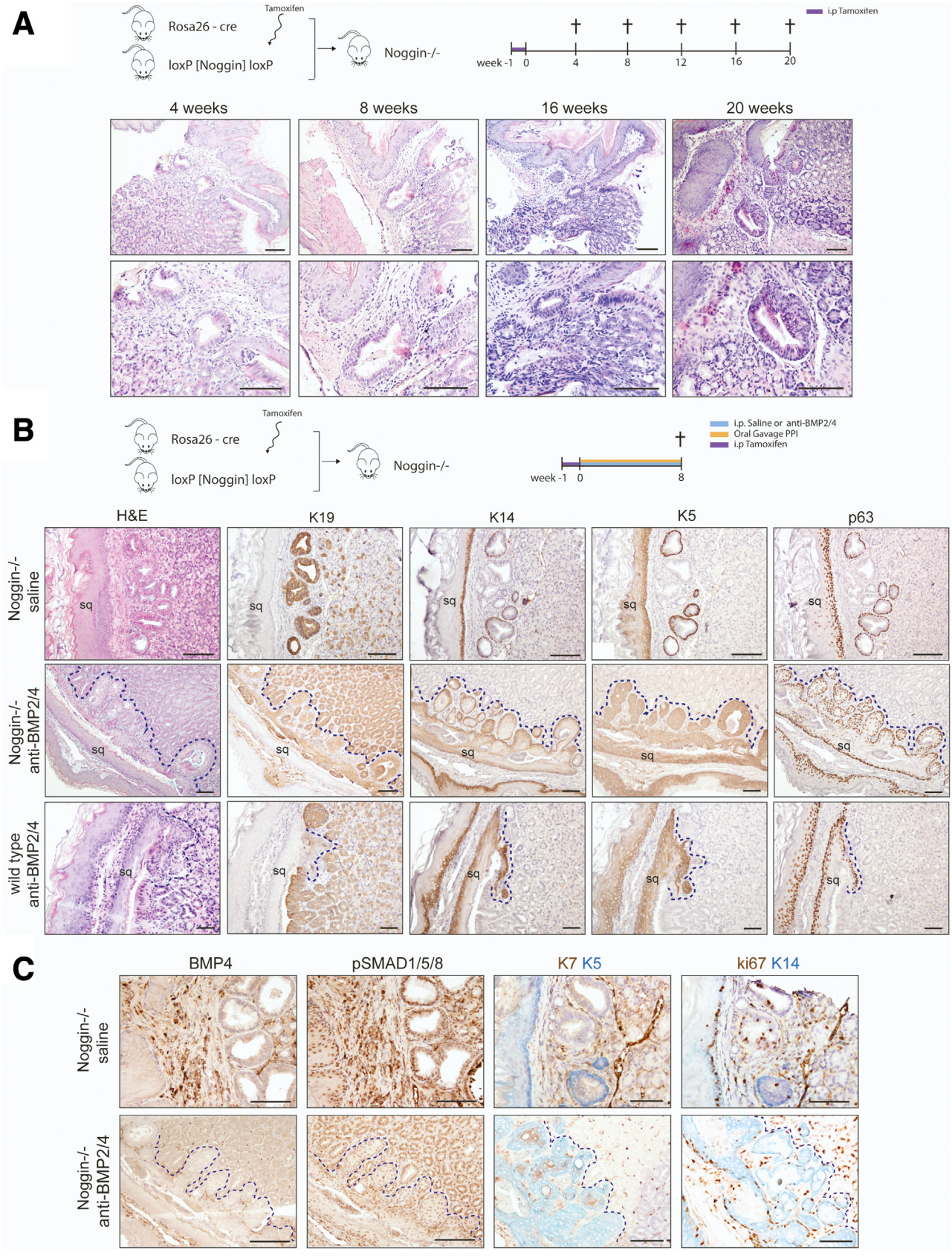
A
Rosa26 - cre
loxP [Noggin] loxP
Tamoxifen
Noggin-/-
i.p Tamoxifen
week -1 0 4 8 12 16 20
4 weeks
8 weeks
16 weeks
20 weeks
B
Rosa26 - cre
loxP [Noggin] loxP
Tamoxifen
Noggin-/-
i.p. Saline or anti-BMP2/4
Oral Gavage PPI
i.p Tamoxifen
week -1 0 8
H&E
K19
K14
K5
p63
Noggin-/- saline
Noggin-/- anti-BMP2/4
wild type anti-BMP2/4
sq
C
BMP4
pSMAD1/5/8
K7 K5
ki67 K14
Noggin-/- saline
Noggin-/- anti-BMP2/4

group) or anti-BMP2/4 (500 μg/mL, daily; treatment group).[23]

K5+ Lineage Tracing Mouse Model

K5-GFP mice were generated by crossing Rosa26-Tomato-loxP [stop] loxP-GFP purchased from the Jackson Laboratory with K5-cre/ERT2 mice, donated by Dr Chen.[39] Genotyped positive K5-GFP mice were housed in individual ventilated cages (+/+ IVC) in ventilated racks in the ARIA. Experiments were performed on 12-week-old mice, both female and male. A total of 8 mice were included of which 7 could be analyzed: control (n = 3) and treated (n = 4). To induce lineage tracing of K5 cells, mice received intraperitoneal injection of tamoxifen (0.25 mg; Sigma-Aldrich) 1 day before the ablation procedure. The stomachs of the K5-GFP mice were ablated as described above. For 14 days, mice received daily oral gavage of omeprazole (400 mol/kg, Teva Pharmaceuticals) and intraperitoneal injection of either saline (control group) or anti-BMP2/4 (500 μg/mL, daily; treatment group).

RNA Extraction and Polymerase Chain Reaction Array of Human Biopsies

Purified human tissue RNA was analyzed using RT^2 Profiler PCR Arrays for human TGF-β/BMP signaling pathway and human hedgehog signaling pathway (Qiagen), according to manufacturer's protocol. After RNA extraction of human tissue specimens, either from the normal squamous epithelium (n = 10) or from the Barrett's epithelium (n = 11), and genomic DNA elimination, cDNA was synthesized from 1 μg of total RNA using RT2 First Strand Kit (Qiagen). cDNA templates were mixed with the polymerase chain reaction (PCR) master mix, samples were aliquot in equal volumes to the plates, and real-time PCR cycling programs were run. For the hedgehog signaling array, the online RT^2 Profiler PCR Array Data Analysis tool from Qiagen was used for normalization and calculation of fold changes and *P* values when comparing the 2 subgroups of samples, Barrett's and squamous tissue. For the TGF-β/BMP array, RNA starting concentrations per sample were calculated using the LinRegPCR tool and visualized in a heatmap.

Cell Lines

The human hTERT immortalized esophageal cell line (EPC2-hTERT) was a gift of Prof Rustgi (University of Pennsylvania, Philadelphia, PA).[40] Primary mouse esophageal keratinocytes cultures were established following the protocol of Kalabis et al.[41] The non-dysplastic Barrett cell line CP-A was provided by Dr R. C. Fitzgerald (University of Cambridge, Cambridge, UK) and used with the permission of Prof P. S. Rabinovitch (University of Washington, WA).[42] All cells were maintained in keratinocyte serum-free medium (Invitrogen) supplemented with 100 U/mL penicillin (Invitrogen), 100 μg/mL streptomycin (Invitrogen), 30 μg/mL bovine pituitary extract, and 0.2 ng/mL human recombinant epidermal growth factor (Invitrogen). All cells were cultured in 5% CO_2 incubator at 37°C and maintained with a weekly passage/refreshing medium. Cells were harvested with trypsin-EDTA, and soybean trypsin inhibitor (Gibco) was used to neutralize trypsin-EDTA effect.

RNA Extraction and Quantitative PCR of Mouse and Human Cell Lines

Total RNA from mouse keratinocytes, human EPC2-hTERT cells, and human Barrett's CP-A cells was extracted with Trizol reagent (Invitrogen) according to the manufacturer's instructions. In all sample types, RNA concentrations were measured using NanoDrop (Thermo Fisher Scientific), with the displayed 260/280 ratios above 1.8 and 260/230 ratios above 1.7.

For mouse and human cell lines, the Reverse Transcription System (Promega) was used, both according to manufacturer's specifications. Gene expression was normalized to the baseline expression levels of corresponding control cells at each treatment time (dashed horizontal line). HPRT1 was used as the reference gene. The relative gene mRNA expression level was determined by the 2-ΔΔct method by quantitative PCR using FastStart SYBR Green Master (Roche) on a Quantica Real Time PCR Thermal Cycler (Techne). Primers used are described in Table 1.

Bioinformatics Analysis

Gene expression profiles of BE and esophageal squamous epithelium were downloaded from the Gene Expression Omnibus (accession number GSE26886).[29] Data were generated using Affymetrix Human Genome U133 Plus 2.0 Array and already pre-processed by use of the GCRMA algorithm. In this set, gene expression was compared between 20 specimens containing cells from Barrett's biopsies obtained through laser capture microdissection and 19 specimens of squamous epithelium from healthy individuals. Chip annotation file GPL570-55999 was used for annotation of the probesets. First, data were filtered using the nsFilter

Figure 7. (***See previous page***). **Effects of BMP2/4 inhibition on neo-columnar epithelium development in a conditional noggin knockout Barrett's model.** (*A*) Rosa26-creERT2 mice were crossed with loxP [Noggin] loxP mice and injected with tamoxifen for 3 days to obtain tamoxifen-inducible noggin$^{-/-}$ mice. H&E of SCJ in the stomach of the tamoxifen-inducible noggin$^{-/-}$ mice at 4, 8, 16, and 20 weeks. (*B*) Creation of tamoxifen-inducible noggin$^{-/-}$ mice and scheme for treatment by saline or anti-BMP2/4 antibody. All mice received proton pump inhibitors (PPIs). H&E and IHC staining of K19, K14, K5, and p63 of the multi-lineage glands at the SCJ in the stomach of wild-type and tamoxifen-inducible noggin$^{-/-}$ mice, treated with anti-BMP2/4 or saline. (*C*) IHC for BMP4, pSMAD1/5/8, K7/K5, and Ki67/K14 of multi-lineage glands at the SCJ in tamoxifen-inducible noggin$^{-/-}$ mice treated with saline or anti-BMP2/4. Hematoxylin was used as a counterstain. (Scale bar: 100 μm) (*broken line* indicates the border of the neo-squamous epithelium).

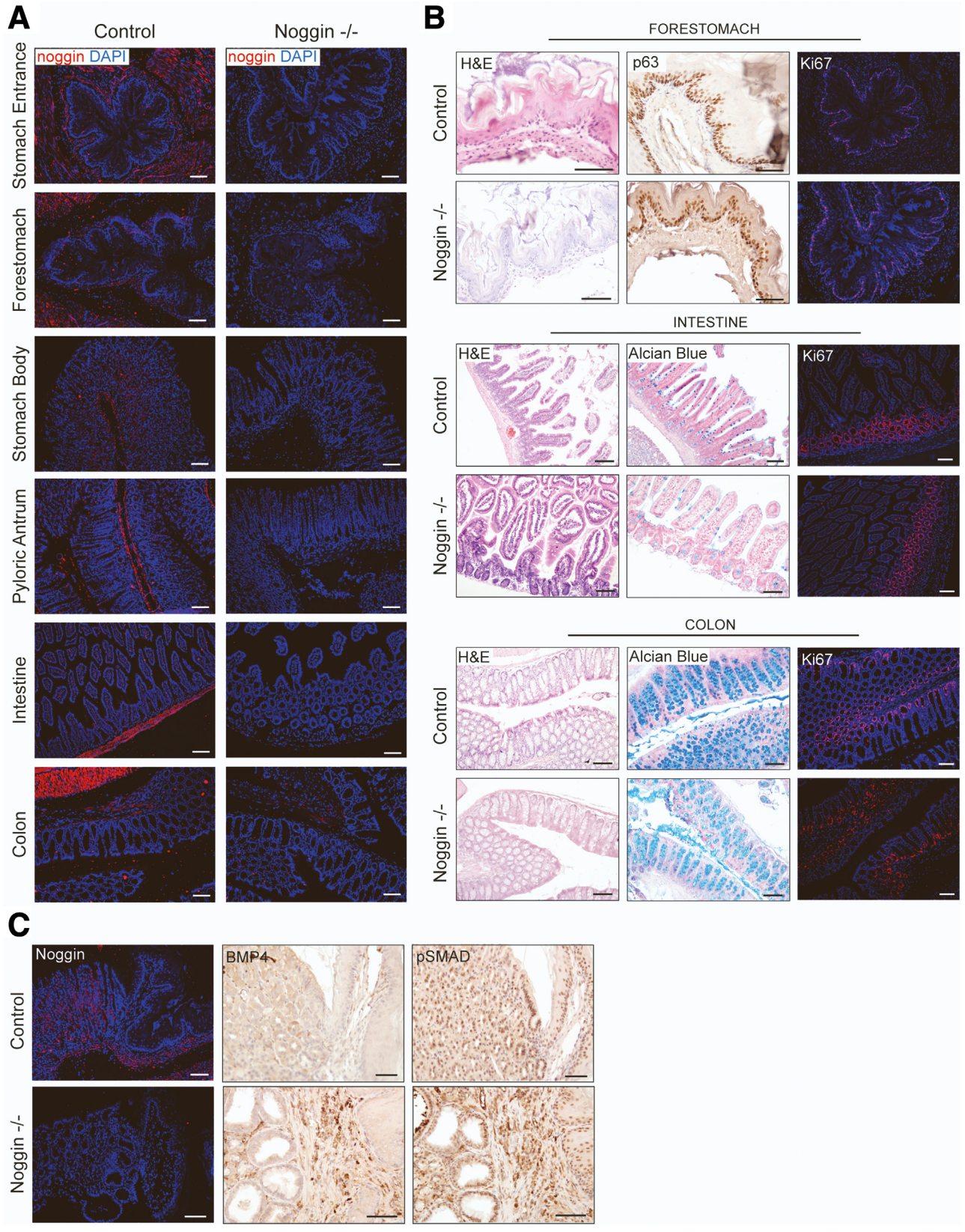

Figure 8. Tamoxifen-inducible noggin knockout (noggin$^{-/-}$) mice injected with tamoxifen for 3 days (intraperitoneally) and compared with control mice (noggin$^{-/-}$ without tamoxifen injection). (*A*) The stomach entrance, forestomach, stomach body, antrum, intestine, and colon were stained for noggin by immunofluorescence and counterstained with DAPI. (*B*) Immunofluorescence for BMP4 and noggin of the SCJ, 24 weeks after tamoxifen injection. Hematoxylin and DAPI were used as counterstain. (*C*) IHC of p63 and ki67 of the forestomach. Alcian blue staining and IHC for ki67. Hematoxylin or DAPI was used as counterstains. (Scale bar: 100 μm).

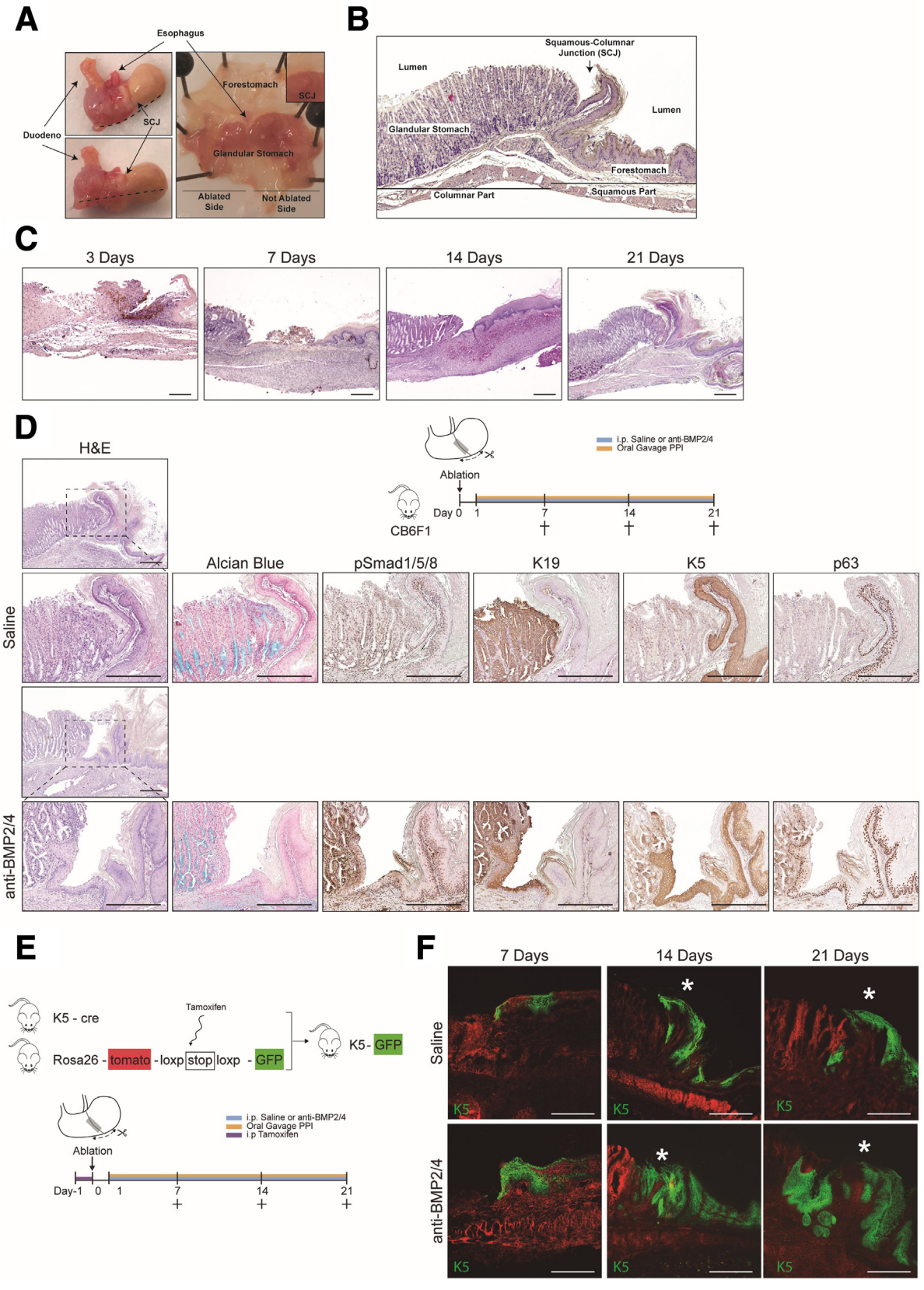
A
Esophagus
Duodeno
SCJ
Forestomach
SCJ
Glandular Stomach
Ablated Side
Not Ablated Side
B
Squamous-Columnar Junction (SCJ)
Lumen
Lumen
Glandular Stomach
Forestomach
Columnar Part
Squamous Part
C
3 Days
7 Days
14 Days
21 Days
D
H&E
i.p. Saline or anti-BMP2/4
Oral Gavage PPI
Ablation
CB6F1
Day 0 1 7 14 21
Alcian Blue
pSmad1/5/8
K19
K5
p63
Saline
anti-BMP2/4
E
K5 - cre
Tamoxifen
Rosa26 - tomato - loxp stop loxp - GFP
K5 - GFP
i.p. Saline or anti-BMP2/4
Oral Gavage PPI
i.p Tamoxifen
Ablation
Day-1 0 1 7 14 21
F
7 Days
14 Days
21 Days
Saline
anti-BMP2/4
K5

Table 1. List of the Primers (Sense and Antisense) Used for Quantitative PCR

Species	Gene name	Sense and antisense
Mouse	*BMP2*	5′-CACACAGGGACACACCAACC-3′
		5′-CAAAGACCTGCTAATCCTCAC-3′
	BMP4	5′-GCCCTGCAGTCCTTCGCTGG-3′
		5′-CTGACGTGCTGGCCCTGGTG-3′
	BMP5	5′-ACCTCTTGCCAGCCTACATG-3′
		5′-TGCTGCTGTCACTGCTTCTC-3′
	BMP7	5′-GTGACCGCAGCCGAATTCAG-3′
		5′-CAACCAGCCCTCCTCAGAAG-3′
	SHH	5′-AATGCCTTGGCCATCTCTGT-3′
		5′-GCTCGACCCTCATAGTGTAGA GAC-3′
	HPRT1	5′-CAACGGGGGACATAAAAGTTA TTGGTGGA-3′
		5′-TGCAACCTTAACCATTTTGGG GCTGT-3′
Human	*BMP2*	5′-AGACCTGTATCGCAGGCACT-3′
		5′-AAACTCCTCCGTGGGGATAG-3′
	BMP4	5′-GATCCACAGCACTGGTCTTG-3′
		5′-GGGATGCTGCTGAGGTTAAA-3′
	BMP5	5′-CGCATACAGTTATCTCG-3′
		5′-CTTTGTAATGCCTTCG-3′
	BMP6	5′-CGTGAAGGCAATGCTCACCT-3′
		5′- CCTGTGGCGTGGTATGCTGT-3′
	BMP7	5′-AGCCCGGGTAGCGCGTAGAG-3′
		5′-GCGCCGGTGGATGAAGCTCGA-3′
	SHH	5′-GCTCGGTGAAAGCAGAGAAC-3′
		5′-CCAGGAAAGTGAGGAAGTCG-3′
	HPRT1	5′-TGACACTGGCAAAACAATGCA-3′
		5′-GGTCCTTTTCACCAGCAAGCT-3′

function from the genefilter package (R package version 1.60.0).[43] Sixty-two control probesets and 27,307 probesets with low variance were removed. Thereafter, differential expression analysis was performed using the limma package.[44] Probesets with multiple-test corrected *P* value. Genes and log2 fold changes were uploaded in IPA, and gene set enrichment analysis for the TGF-β/BMP/SHH pathways was performed. The TGF-β signaling pathways were visualized using Path Designer.

A gene-clustered heatmap was drawn for quantitative PCR data from the AMC data set using the heatmap package after log transformation and calculation of z-scores for all samples per gene.

A similar gene-clustered heatmap was drawn for the Wang database after calculating z-scores for all samples per gene. In case of multiple significantly differentially expressed probesets coding for the same gene, mean expression of these probesets was used as expression value of that particular gene.

Western Blot of Human Biopsies

After dissecting, tissue biopsies (n = 6 per tissue type) were briefly washed with cold phosphate-buffered saline and cut into smaller pieces while on ice. Minced tissue was transferred to a homogenizer, and 500 μL of RIPA buffer (Thermo Fisher Scientific) supplemented with protease inhibitors (Thermo Fisher Scientific) was added per 10 mg of tissue. Samples were carefully homogenized and kept on ice for 30 minutes while mixing occasionally. Subsequently, samples were sonicated for 2–5 minutes and centrifuged at 10,000*g* for 20 minutes at 4°C. The supernatant was transferred to a new tube and stored at –20°C until future use. Protein concentrations were determined using the Pierce BCA Protein Assay Kit (Pierce Biotechnology), following the manufacturer's protocol. Lysates were combined with sample buffer (125 mmol/L Tris-HCl, pH 6.8; 4% sodium dodecyl sulfate; 2% β-mercaptoethanol; 20% glycerol; 1 mg bromophenol blue) and loaded with the equal amount of protein (15 μg/lane) on a 12% sodium dodecyl sulfate-polyacrylamide gel and subsequently blotted onto polyvinylidene difluoride transfer membranes (Millipore). The membranes were blocked with blocking solution (5% nonfat milk in Tris-buffered saline with 1% Tween-20) and afterwards incubated with the appropriate primary antibody solution anti-BMP2 (Peprotech), anti-BMP4 (R&D), anti-BMP5 (Abcam), and anti-BMP6 (R&D) at a 1:500 dilution in blocking solution overnight at 4°C. Subsequently, membranes were washed and incubated with secondary antibodies, horseradish peroxidase-anti-goat (Dako), horseradish peroxidase-anti-rabbit (Dako), and horseradish peroxidase-anti-mouse (Dako), diluted 1:2000 in blocking solution for 1 hour at room temperature. Membranes were incubated with Pierce enhanced chemiluminescent substrate (Pierce Biotechnology), and proteins were visualized using ImageQuant LAS 4000 (GE Healthcare Life Science). Densitometry analysis was performed using Image J 1.45s (Wayne Rasband).

Immunohistochemistry

Formalin-fixed, paraffin-embedded tissue samples were used for immunohistochemistry. Slides with 5-μm-thick sections from the paraffin blocks were cut and deparaffinized in xylene and rehydrated in a graded series of ethanol. Antigen

Figure 9. (***See previous page***). **Anti-BMP2/4 treatment and lineage tracing of K5+ progenitor cells in a cryoablation model of premalignant columnar lesions.** (*A*) Macroscopic view of a dissected wild-type CB6F1/Crl mouse stomach, 21 days after ablation of a glandular part of the stomach. (*B*) H&E staining of a normal SCJ, including both the forestomach and glandular stomach of wild-type mice. (*C*) H&E of the SCJ of wild-type mice after 3, 7, 14, or 21 days of cryoablation of the glandular stomach epithelium. (*D*) Cryoablation and scheme for treatment with saline or anti-BMP2/4. All mice received PPIs. H&E, Alcian blue staining, and IHC for pSMAD1/5/8, K19, K5, and p63 of the SCJ in CB6F1/Crl mice, 21 days after cryoablation and treatment with saline or anti-BMP2/4. Hematoxylin was used as a counterstain. (*E*) Crossing of K5-cre mice with Rosa26-Tomato-lox-stop-loxGFP mice and injection with tamoxifen to generate K5-GFP lineage-tracing mice. Cryoablation and scheme for treatment with saline or anti-BMP2/4. (*F*) GFP expressing squamous cells traced in K5-GFP mice after cryoablation of the columnar epithelium in the proximal stomach at the SCJ (*) in mice treated with saline or anti-BMP2/4. (Scale bar: 200 μm).

retrieval was performed in citrate buffer saline (0.01 mol/L, pH 6.0) for 20 minutes at 98°C. Endogenous peroxidase activity was blocked by incubation of slides in 3% H_2O_2 for 30 minutes, followed by 10% normal goat serum for 30 minutes to block nonspecific binding. Slides were incubated at room temperature for 2 hours or overnight at 4°C with primary antibodies: anti-BMP2 (1:100, LifeSpan BioSciences), anti-BMP4 (1:400, Abcam), anti-CDX2 (1:200, Biogenex), anti-mitochondria (1:1000, Abcam), anti-Involucrin (1:100, Covalab), anti-K5 (1:200, Abcam), anti-K14 (1:200, Abcam), anti-K19 (1:200, Epitomics), anti-Ki67 (1:200, Thermo Fisher Scientific), anti-p63 (1:100, Santa Cruz Biotechnology), anti-pSmad 1/5/8 (1:100, Merck Millipore), anti-SOX2 (1:200, Epitomics), anti-MUC5AC (1:100, Thermo Fisher Scientific), and anti-noggin (1:100, Epitomics). Slides were washed in Tris-buffered saline + 1% Tween 20 and incubated with the respective biotin linked secondary reagents from the LSAB 2 Kits (Dako) following the manufacturer's protocol. Peroxidase activity was visualized using DAB+ (Dako). Finally, sections were counterstained with Mayer's hematoxylin, dehydrated, and mounted.

Mouse Models Power Analysis

All mice used in this article were mostly pilot/feasibility studies. For the in vivo organoid model of human BE biopsies and cryoablation mouse model of premalignant columnar lesions, the power calculation performed was as follows: 2-sided *t* test, alpha: 0.05, reference (control): 1.0; expectation: 2.0; SD: 2.0; power of 0.7, indicated that we needed at least 6 animals per group. An extra 10% of animals was included to compensate for animal loss due to procedures. To minimize the use of animals, the number of control wild-type animals in the cryoablation mouse model could be reduced because of the availability of aged/sex matched historical controls (normal phenotypes).

For the cryoablation of lineage tracing K5+ progenitor cells study, the expected effect could be better predicted. The power calculation was as follows: 2-sided *t* test, alpha: 0.05, reference: 1.0; expectation: 4.0; SD: 2.0; power of 0.8, indicated that we needed 4 animals per group.

For the tamoxifen-inducible noggin knockout mice the following power calculation was performed: 2-sided *t* test, alpha: 0.05, reference (control): 1.0; expectation: 3.0; SD:2.0; power of 0.8, indicated 8 animals were needed per group. To minimize animal use and evaluate effects over time, each of the group of 8 animals were killed at 2 time points (eg, group 1: at 4 (n = 4) and 8 weeks (n = 4); group 2 at 12 (n = 4) and 16 weeks (n = 4).

Statistics

Quantitative PCR data were tested for a normal distribution using the Shapiro test. The Mann-Whitney *U* test was performed to investigate differences in expression of each gene between BE and normal squamous tissue for the PCR arrays. Genes with $P < .05$ were considered differentially expressed. Statistical differences in protein level were determined using Kruskal-Wallis test in a multiple comparison 1-way analysis of variance. Two-sided paired *t* tests were performed to test statistical differences in mRNA expression of BMP2, BMP4, BMP7, and SHH in cells treated with bile acids at different time points. Statistical significance was set at $P < .05$. Unpaired *t* test: $^*P < .0001$.

References

1. Spechler SJ. Barrett's esophagus and esophageal adenocarcinoma: pathogenesis, diagnosis, and therapy. Med Clin North Am 2002;86:1423–1445, vii.
2. Souza RF. From reflux esophagitis to esophageal adenocarcinoma. Dig Dis 2016;34:483–490.
3. DeMeester TR. Antireflux surgery in the management of Barrett's esophagus. J Gastrointest Surg 2000; 4:124–128.
4. Spechler SJ, Sharma P, Souza RF, et al. American Gastroenterological Association technical review on the management of Barrett's esophagus. Gastroenterology 2011;140:e18–e52, quiz e13.
5. Peters Y, Al-Kaabi A, Shaheen NJ, et al. Barrett oesophagus. Nat Rev Dis Primers 2019;5:35.
6. Coleman HG, Xie SH, Lagergren J. The epidemiology of esophageal adenocarcinoma. Gastroenterology 2018; 154:390–405.
7. Read MD, Krishnadath KK, Clemons NJ, et al. Preclinical models for the study of Barrett's carcinogenesis. Ann N Y Acad Sci 2018;1434:139–148.
8. Visrodia K, Zakko L, Wang KK. Mucosal ablation in patients with Barrett's esophagus: fry or freeze? Dig Dis Sci 2018;63:2129–2135.
9. Singh T, Sanaka MR, Thota PN. Endoscopic therapy for Barrett's esophagus and early esophageal cancer: where do we go from here? World J Gastrointest Endosc 2018; 10:165–174.
10. Bragdon B, Moseychuk O, Saldanha S, et al. Bone morphogenetic proteins: a critical review. Cell Signal 2011;23:609–620.
11. Auclair BA, Benoit YD, Rivard N, et al. Bone morphogenetic protein signaling is essential for terminal differentiation of the intestinal secretory cell lineage. Gastroenterology 2007;133:887–896.
12. Gomez-Puerto MC, Iyengar PV, Garcia de Vinuesa A, et al. Bone morphogenetic protein receptor signal transduction in human disease. J Pathol 2019;247:9–20.
13. Que J, Choi M, Ziel JW, et al. Morphogenesis of the trachea and esophagus: current players and new roles for noggin and Bmps. Differentiation 2006;74:422–437.
14. Piccolo S, Sasai Y, Lu B, et al. Dorsoventral patterning in Xenopus: inhibition of ventral signals by direct binding of chordin to BMP-4. Cell 1996;86:589–598.
15. Zimmerman LB, De Jesus-Escobar JM, Harland RM. The Spemann organizer signal noggin binds and inactivates bone morphogenetic protein 4. Cell 1996;86:599–606.
16. Milano F, van Baal JW, Buttar NS, et al. Bone morphogenetic protein 4 expressed in esophagitis induces a columnar phenotype in esophageal squamous cells. Gastroenterology 2007;132:2412–2421.
17. Jiang M, Ku WY, Zhou Z, et al. BMP-driven NRF2 activation in esophageal basal cell differentiation and

eosinophilic esophagitis. J Clin Invest 2015; 125:1557–1568.
18. Wang DH, Tiwari A, Kim ME, et al. Hedgehog signaling regulates FOXA2 in esophageal embryogenesis and Barrett's metaplasia. J Clin Invest 2014;124:3767–3780.
19. Mari L, Milano F, Parikh K, et al. A pSMAD/CDX2 complex is essential for the intestinalization of epithelial metaplasia. Cell Rep 2014;7:1197–1210.
20. Clemons NJ, Wang DH, Croagh D, et al. Sox9 drives columnar differentiation of esophageal squamous epithelium: a possible role in the pathogenesis of Barrett's esophagus. Am J Physiol Gastrointest Liver Physiol 2012;303:G1335–G1346.
21. Zhou G, Sun YG, Wang HB, et al. Acid and bile salt upregulate BMP4 expression in human esophageal epithelium cells. Scand J Gastroenterol 2009;44:926–932.
22. Quante M, Bhagat G, Abrams JA, et al. Bile acid and inflammation activate gastric cardia stem cells in a mouse model of Barrett-like metaplasia. Cancer Cell 2012;21:36–51.
23. Calpe S, Wagner K, El Khattabi M, et al. Effective inhibition of bone morphogenetic protein function by highly specific llama-derived antibodies. Mol Cancer Ther 2015; 14:2527–2540.
24. Calpe S, Correia AC, Sancho-Serra Mdel C, et al. Comparison of newly developed anti-bone morphogenetic protein 4 llama-derived antibodies with commercially available BMP4 inhibitors. MAbs 2016;8:678–688.
25. Castillo D, Puig S, Iglesias M, et al. Activation of the BMP4 pathway and early expression of CDX2 characterize non-specialized columnar metaplasia in a human model of Barrett's esophagus. J Gastrointest Surg 2012; 16:227–237, discussion 237.
26. Zhang Y, Wang Y, Yang K, et al. BMP4 increases the expression of TRPC and basal [Ca2+]i via the p38MAPK and ERK1/2 pathways independent of BMPRII in PASMCs. PLoS One 2014;9:e112695.
27. Wang Q, Ma C, Kemmner W. Wdr66 is a novel marker for risk stratification and involved in epithelial-mesenchymal transition of esophageal squamous cell carcinoma. BMC Cancer 2013;13:137.
28. Straub D, Oude Elferink RPJ, Jansen PLM, et al. Glycoconjugated bile acids drive the initial metaplastic gland formation from multi-layered glands through crypt-fission in a murine model. PLoS One 2019;14:e0220050.
29. Wang Q, Ma C, Kemmner W. Wdr66 is a novel marker for risk stratification and involved in epithelial-mesenchymal transition of esophageal squamous cell carcinoma. BMC Cancer 2013;13:137.
30. Costamagna D, Mommaerts H, Sampaolesi M, et al. Noggin inactivation affects the number and differentiation potential of muscle progenitor cells in vivo. Sci Rep 2016;6:31949.
31. Brunet LJ, McMahon JA, McMahon AP, et al. Noggin, cartilage morphogenesis, and joint formation in the mammalian skeleton. Science 1998;280:1455–1457.
32. Jiang M, Li H, Zhang Y, et al. Transitional basal cells at the squamous-columnar junction generate Barrett's oesophagus. Nature 2017;550:529–533.
33. Correia ACP, Straub D, Calpe S, et al. Novel in vivo mouse cryoablation model to explore unique therapeutic approaches for premalignant columnar lesions. Methods Protoc 2021;4.
34. Pavlov K, Meijer C, van den Berg A, et al. Embryological signaling pathways in Barrett's metaplasia development and malignant transformation: mechanisms and therapeutic opportunities. Crit Rev Oncol Hematol 2014; 92:25–37.
35. Barros R, Pereira B, Duluc I, et al. Key elements of the BMP/SMAD pathway co-localize with CDX2 in intestinal metaplasia and regulate CDX2 expression in human gastric cell lines. J Pathol 2008; 215:411–420.
36. Daniely Y, Liao G, Dixon D, et al. Critical role of p63 in the development of a normal esophageal and tracheobronchial epithelium. Am J Physiol Cell Physiol 2004; 287:C171–C181.
37. Hall PA, Woodman AC, Campbell SJ, et al. Expression of the p53 homologue p63alpha and DeltaNp63alpha in the neoplastic sequence of Barrett's oesophagus: correlation with morphology and p53 protein. Gut 2001; 49:618–623.
38. Krause C, Guzman A, Knaus P. Noggin. Int J Biochem Cell Biol 2011;43:478–481.
39. Liang CC, You LR, Chang JL, et al. Transgenic mice exhibiting inducible and spontaneous Cre activities driven by a bovine keratin 5 promoter that can be used for the conditional analysis of basal epithelial cells in multiple organs. J Biomed Sci 2009;16:2.
40. Harada H, Nakagawa H, Oyama K, et al. Telomerase induces immortalization of human esophageal keratinocytes without p16INK4a inactivation. Mol Cancer Res 2003;1:729–738.
41. Kalabis J, Wong GS, Vega ME, et al. Isolation and characterization of mouse and human esophageal epithelial cells in 3D organotypic culture. Nat Protoc 2012;7:235–246.
42. Palanca-Wessels MC, Klingelhutz A, Reid BJ, et al. Extended lifespan of Barrett's esophagus epithelium transduced with the human telomerase catalytic subunit: a useful in vitro model. Carcinogenesis 2003; 24:1183–1190.
43. Gentleman RCV, Huber W, Hahne F. Genefilter: methods for filtering genes from high-throughput experiments. R package version 1.60.0 2017.
44. Ritchie ME, Phipson B, Wu D, et al. limma powers differential expression analyses for RNA-sequencing and microarray studies. Nucleic Acids Res 2015; 43:e47.

Received May 24, 2021. Accepted January 17, 2023.

Correspondence
Address correspondence to: Sheila K. Krishnadath, MD, PhD, Laboratory of Experimental Medicine and Paediatrics, Antwerp University, Universiteitsplein 1, 2610 Antwerp, Belgium. e-mail: Sheila.Krishnadath@UZA.be; or Ana C. P. Correia, PhD, Center of Experimental and Molecular Medicine, University of Amsterdam, Meibergdreef 9, 1105 AZ Amsterdam, The Netherlands. e-mail: a.c.pachecocorreia@amsterdamumc.nl.

CRediT Authorship Contributions

Ana C. P. Correia, PhD candidate (Conceptualization: Equal; Formal analysis: Lead; Investigation: Equal; Methodology: Lead; Validation: Lead; Writing – original draft: Lead; Writing – review & editing: Equal)

Danielle Straub, PhD (Conceptualization: Equal; Formal analysis: Lead; Investigation: Equal; Methodology: Lead; Writing – original draft: Lead; Writing – review & editing: Supporting)

Matthew Read, MD, PhD (Methodology: Equal; Writing – review & editing: Supporting)

Sanne J. M. Hoefnagel, MD, PhD candidate (Formal analysis: Equal; Methodology: Supporting; Writing – original draft: Supporting; Writing – review & editing: Supporting)

Salvador Romero-Pinedo, PhD candidate (Investigation: Supporting; Methodology: Equal; Writing – review & editing: Supporting)

Ana C. Abadía-Molina, Prof, PhD (Funding acquisition: Equal; Writing – review & editing: Supporting)

Nicholas J. Clemons, Prof, PhD (Writing – review & editing: Supporting)

Kenneth Wang, Prof, MD, PhD (Conceptualization: Supporting; Writing – review & editing: Supporting)

Silvia Calpe, PhD (Conceptualization: Equal; Formal analysis: Supporting; Supervision: Supporting; Writing – original draft: Supporting; Writing – review & editing: Lead)

Wayne Phillips, Prof, PhD (Conceptualization: Supporting; Writing – review & editing: Supporting)

Kausilia K. Krishnadath, Prof, MD, PhD (Conceptualization: Lead; Funding acquisition: Lead; Supervision: Supporting; Writing – review & editing: Lead)

Conflicts of interest

The authors disclose no conflicts.

Funding

Supported by the European Research Council (ERC) starting grant: ERC-StG 282079 TargetS4Barrett, ERC-POC 632258 BMP4EAC, and a Dutch government grant: LSH-TKI-PPP 2017. Plan Estatal de Investigación Científica y Técnica y de Innovación 2013–2016, ISCIII-Subdirección General de Evaluación y Fomento de la Investigación, Ministerio de Economía y Competitividad, Spain (grant PI16/01642 & PI10/01096).